Copper(I) Forms a Redox Stable 1:2 Complex with α-Synuclein N-Terminal Peptide in a Membrane-Like Environment

Simone Dell'Acqua,[†] Valentina Pirota, [†] Enrico Monzani, [†] Francesca Camponeschi,[‡] Riccardo De Ricco, [‡] Daniela Valensin[‡]* and Luigi Casella[†]*

[†] Dipartimento di Chimica, Università di Pavia, Via Taramelli 12, 27100, Pavia, Italy. [‡] Dipartimento di Biotecnologie, Chimica e Farmacia, Università di Siena, Via Aldo Moro 2, 53100, Siena, Italy.

ABSTRACT: α-Synuclein (αS) is the main protein component of Lewy bodies, characterizing the pathogenesis of Parkinson's disease. αS is unstructured in solution but adopts a helical structure in its extended N-terminal segment upon association with membranes. *In vitro* the protein binds avidly Cu^{II}, but *in vivo* the protein is N-acetylated and Cu^{II} binding is lost. We have now clarified the binding characteristics of the Cu^{I} complex with the truncated αS peptide 1-15, both in N-acetylated and free amine forms, in a membrane mimetic environment and found that complexation occurs with a 1:2 Cu^{I}-αS stoichiometry, where Cu^{I} is bound to Met1 and Met5 residues of two helical peptide chains. The resulting tetrahedral Cu^{I} center is redox stable, does not form reactive oxygen species, and is unreactive against dopamine in the presence of O_2. This suggests that, unlike cytosolic Cu^{I}-αS, which retains the capacity to activate O_2 and promote oxidative reactions, membrane-bound Cu^{I}-αS may serve as a sink for unreactive copper.

INTRODUCTION

α-Synuclein (αS) is a small (140-residue), natively unfolded cytosolic protein,[1] constituting the primary component of the intracellular aggregates present in Lewy bodies,[2] a hallmark of Parkinson's disease (PD).[3] The mechanism of formation of these inclusion bodies and their relationship with the specific damage of dopaminergic neurons of the substantia nigra occurring in the disease remain unclear. In addition, αS is found both inside and outside neuronal cells, for instance as the non-amyloid-β component of the extracellular amyloid plaques in Alzheimer's disease brains.[4] Although the normal function of αS remains unknown, its localization at presynaptic terminals[5] and its association with synaptic vesicles[6] suggest that αS has a role in neurotransmitter release, and in particular as a chaperone controlling SNARE protein complex assembly and distribution.[7] The investigation of the structural properties, redox reactivity, ligand and metal binding behavior of αS has been carried out mostly using protein or fragments containing a free amino N-terminal group,[8] whereas *in vivo* the protein is N-acetylated.[9] In addition, it should be taken into account that most αS resides in a membrane environment, whereas the vast majority of *in vitro* studies focused on protein or peptide fragments in solution. In particular, this concerns the metal binding properties of αS, which are relevant because high concentrations of metal ions are detected in Lewy bodies,[10] and in cerebrospinal fluids of PD patients,[11] as a result of abnormal metal homeostasis. Among them, Cu^{II} binding appears to be strongly affected by N-acetylation, as the remarkable affinity of non-acetylated αS for this metal ion, with K_d in the range of 0.1 nM,[12] is completely lost upon N-acetylation.[13] In contrast, binding to Cu^{I} is not affected by this modification, because it occurs at the sulfur atoms of Met1 and Met5 side chains of both N-acetylated and free amine forms of αS.[14]

In this paper, we address the problem of the structure and redox reactivity of the Cu^{I} complex of the αS N-terminal peptide 1-15 in a model membrane, explicitly considering the effect of N-acetylation. It is known that αS becomes partially structured in α-helical form upon interaction with phospholipids, unilamellar vesicles, and sodium dodecyl sulfate (SDS) micelles.[15] N-Acetylation further increases lipid affinity and α-helical propensity of the N terminus.[16] Among the variety of studies carried out with non-acetylated αS, worthy of note in the present context are the differences recently emerged in the behavior of the Cu^{II}-αS complex in a membrane environment compared with aqueous buffer solution. The metal coordination set only loses His50 binding, due to N-terminal α-helix structuring of the peptide, leaving the affinity approximately constant (K_d ~0.1 nM),[17] and the membrane environment favors a reduction in oxygen radicals production.[18] The reactivity studies of the Cu-αS_{1-15} and Cu-Ac-αS_{1-15} complexes are here addressed toward the oxidation of dopamine, and related catechols, in view of its possible interaction with αS at nerve terminals.[3]

RESULTS AND DISCUSSION

To evaluate the structural properties of the Cu^{I} binding region in the membrane mimicking environment, we used the N-terminal αS pentadecapeptide fragment, both in the N-acetylated (Ac-αS_{1-15}) and free amine (αS_{1-15}) forms, containing the coordinating residues for Cu^{I}.[14,19]

Like the full length protein, Ac-αS$_{1-15}$ and αS$_{1-15}$ undergo a conformational transition from random coil to α-helix upon interaction with SDS micelles, as shown by the CD spectra and the 3D NMR structure obtained in presence of membrane mimicking environment (see Figure 1S in Supporting Information). As previously found for the full length protein,[16] our NMR structures show that α-helix conformation is stabilized by N-acetylation of the 15-amino acid peptide. Copper(I) binding to Ac-αS$_{1-15}$ and αS$_{1-15}$ was first investigated through the changes observed in NMR spectra. In addition to experiments performed in presence of Cu^{I}, we also used Ag^{I} as a convenient, redox stable probe, that proved to be helpful to define the metal coordination characteristics of Cu^{I}-αS in aqueous solution.[19a,20] Cu^{I} and Ag^{I} additions to Ac-αS$_{1-15}$ cause selective chemical shift variations on ^{1}H NMR signals. The presence of 0.4 Cu^{I} or Ag^{I} equiv. yields very comparable variations on peptide NMR resonances, as shown in Figure 1, thus supporting similar metal coordination spheres. In both cases, the most affected residues are Met1, Phe4, Met5 and Gly7.

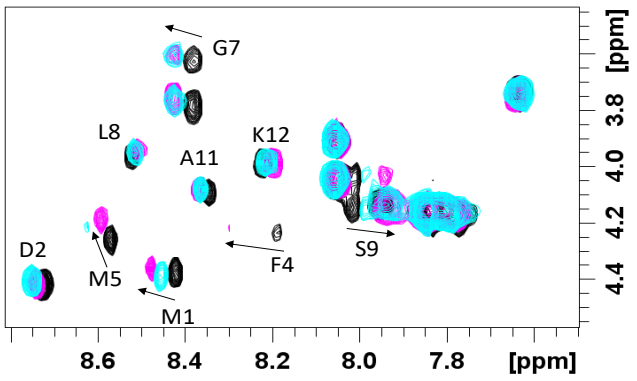

Figure 1. Overlay of ^{1}H-^{1}H TOCSY spectra of Ac-αS$_{1-15}$ in absence (black) and in presence of 0.4 Cu^{I} (cyan) and 0.4 Ag^{I} equiv. (magenta). Peptide concentration was 0.4 mM, in 20 mM phosphate buffer, 40 mM SDS.

Interestingly, besides chemical shift variations, selective line broadening is observed for Phe4 and Met5 correlations. The broadening, also evident in the ^{1}H-^{13}C HSQC peaks of Met1 and Met5 thioether groups, is attenuated by slightly increasing metal concentration (Figure 2S). In addition to that, as normally found in titration experiments, the chemical shift variations become more significant by gradually increasing metal concentration, as shown by the shift of methyl protons of Val3 and Leu8 for both Cu^{I} and Ag^{I} complexes (Figure 2A). We focused on resonances easy to examine for both metal ion titrations belonging to CH_3 groups of Val and Leu since this region is, contrary to amide Met SCH_3 (2.6-1.8 ppm) regions, which are sensitive to minimal variations and obscured by ascorbic acid signals for Cu^{I} containing spectra. Interestingly, Ag^{I} and Cu^{I} provide very similar effects, strongly indicating an analogy in their binding modes. Plotting the measured chemical shift variations shows that a chemical shift plateau is reached in presence of about 0.5 metal equivalents and no changes occur by further increasing metal ion concentration (Figure 2B). This behavior is also evident in similar plots of chemical shift variations of methyl protons of Met1 and Met5 and amide protons of Met1, Asp2, Phe4, Met5 and Leu8 (Figures 3S and 4S), suggesting the formation of a 1:2 metal-peptide complex, where the metal is tetrahedrally coordinated to the four thioether groups of Met1 and Met5 of two helical Ac-αS$_{1-15}$ molecules. The binding plots enabled to obtain estimated K_d values of 2.9×10^{-8} (for Cu^{I}) and 2.6×10^{-8} M^2 (for Ag^{I}) (Figures 2B and 4S), i.e. two orders of magnitude smaller than that found for the complex with the full protein, Cu^{I}-αS, in aqueous buffer.[14] These values were further supported by fitting data shown in Figure 4S, yielding K_d values ranging from 2.5×10^{-8} to 7.7×10^{-8} M^2.

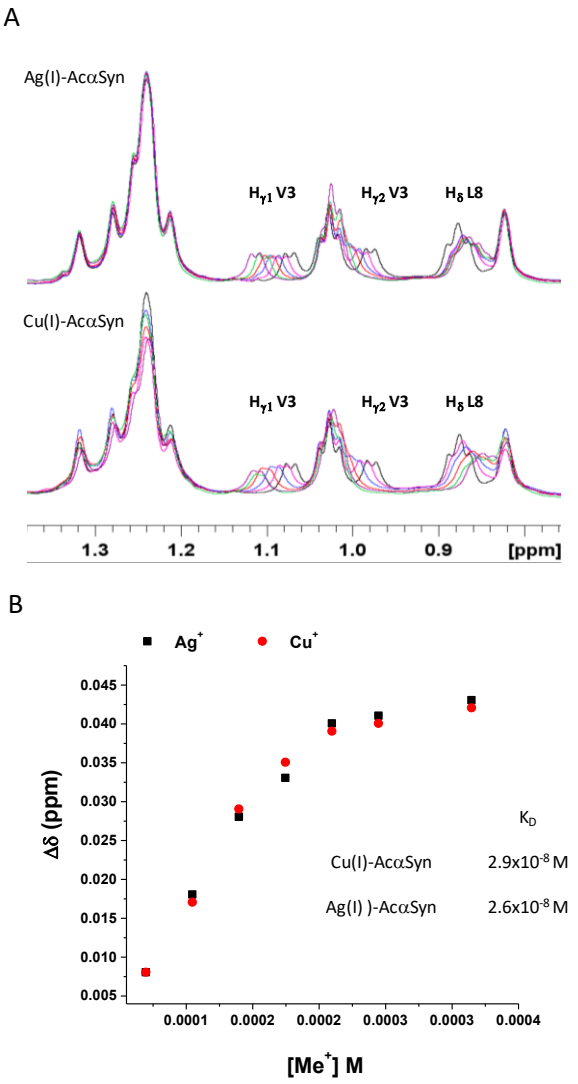

Figure 2. (A). Overlay of selected regions of ^{1}H NMR spectra of Ac-αS1-15 0.4 mM with increasing amount of Cu^{I} (lower panel) and Ag^{I} (upper panel): from 0.0 (black trace) to 0.5 (violet trace) Ag^{I} equiv.; (B) Binding curves of Ag^{I}-Ac-αS$_{1-15}$ (black squares) and Cu^{I}-AcαS$_{1-15}$ (red circles) complexes as monitored by changes

in methyl protons chemical shifts (Δδ) of Val3. Peptide concentration was 0.4 mM, in phosphate buffer 20 mM, 40 mM SDS.

Interestingly, identical behavior (Figures 5S, 6S and 7S) was observed for $\alpha S_{1\text{-}15}$, strongly indicating that the metal coordination sphere and stoichiometry is maintained regardless of the presence of N-acetylated or free amine N-terminus.

The *i* and *i+4* positions of the two methionines in the αS sequence make their side chains perfectly positioned one above the other in an α-helical structure. Therefore, it can be anticipated that Cu^I, or Ag^I, binding to Met1 and Met5 is stabilized by the helical conformation of the peptide. In fact, CD spectra of Ac-$\alpha S_{1\text{-}15}$ recorded in presence of either Cu^I or Ag^I confirm that the peptide backbone retains the α-helical conformation (Figure 8S). In addition, the comparison of NMR spectra of apo and metal bound Ac-$\alpha S_{1\text{-}15}$ confirms the maintenance of all H_N-H_N NOEs, typical of systems containing α-helical structure (Figure 3).

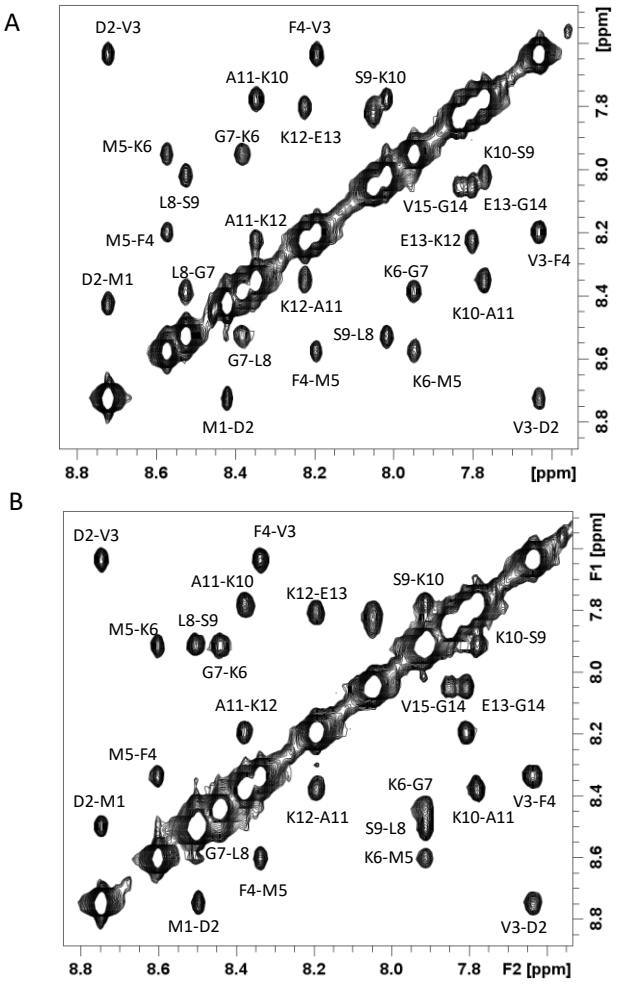

Figure 3. Selected regions of ^{1}H-^{1}H NOESY spectra of Ac-$\alpha S_{1\text{-}15}$ in the absence (A) or presence of 0.6 Ag^I metal equiv. Peptide concentration was 0.4 mM, in phosphate buffer 20 mM, 40 mM SDS.

NOEs cross-peaks belonging to Ag^I-Ac-$\alpha S_{1\text{-}15}$ complexes were converted into proton-proton distances to be used as restraints for the structure determination (see experimental section for details). The obtained structures (Figure 9S) are well superimposed and support a well-defined α-helix conformation from residue 1 to 12. On the other hand, two opposite orientations are found for the metal ion, which appears to assume a tetrahedral geometry. These data are in agreement with the NMR titration experiments shown in Figure 2 and strongly support the formation of a bis-peptide complex.

The obtained structural features were then exploited to build up a model of the Cu^I-$\alpha S_{1\text{-}15}$ complex (Figure 4), considering the effective 1:2 Cu:peptide stoichiometry and imposing Cu^I-sulfur distances in the range of 2.15-2.35 Å for all four Met ligands. To generate this model we considered the same H-H distance restrains for both monomers. Figure 4 shows the existence of two possible relative orientations of two α-helical peptides, containing the N- and C-termini parallel or antiparallel to each other, respectively. The proposed Cu(I) binding sites include 4 sulfur donor atoms and show different solvent accessibility. CPK graphical representation of the mean structures corresponding to parallel or antiparallel conformations, point out that copper ions are less solvent exposed when the dimeric Cu^I -$\alpha S_{1\text{-}15}$ structure is antiparallel (Figure 10S).

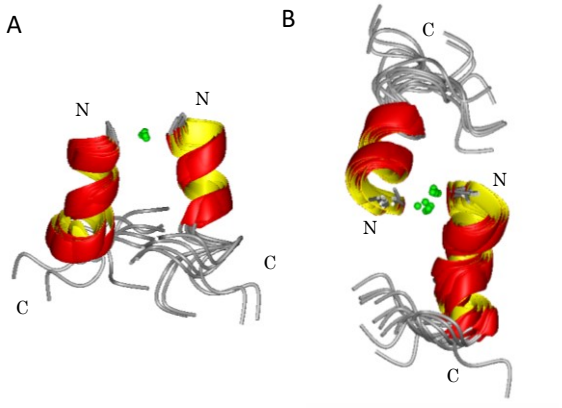

Figure 4. Structural models of Cu^I-Ac-$\alpha S_{1\text{-}15}$ 1:2 complex. The structures were fitted on the 1-10 backbone residues of the two Ac-$\alpha S_{1\text{-}15}$ molecules. (A) The first 10 structures with parallel orientation of the helices, RMSD values of 0.86 ± 0.37 Å and 1.45 ± 0.49 Å for backbone and heavy atoms, respectively. (B) The first 14 structures with antiparallel orientation of the helices, RMSD values of 1.49 ± 0.62 Å and 2.15 ± 0.67 Å for backbone and heavy atoms. Figure was created with MOLMOL 2.K.1.

The importance of oxidative modifications of αS in determining structural/biological alterations of the protein is well recognized,[21] and the effects associated with metal binding to αS are of particular relevance in this context. The possibility that metal-αS complexes produce oxygen radicals is also worthy of note,[18] because these species may be toxic also to exogenous molecules. We therefore performed a series of experiments with the aim of assessing the effect of membrane incorporation of the Cu^I-Ac-$\alpha S_{1\text{-}15}$ complex, and the parent Cu^I-$\alpha S_{1\text{-}15}$ complex, on their oxidative reactivity towards external substrates. Among the potential substrates, the most important is

certainly dopamine (DA), in view of the possible involvement of αS in the control of the neurotransmitter cytoplasmic concentration and release at nerve terminals,[3] and the observation that *in vitro* DA oxidation induces formation of stable, potentially toxic αS oligomers.[22] However, DA itself is not an easily manageable substrate to obtain quantitative information: its oxidation is slow in the presence of catalytic amounts of Cu^{II},[23] while the corresponding quinone (DAQ) is very reactive and undergoes rapid conversion to dopaminochrome (DAC) and further oxidative oligomerization,[24] yielding insoluble melanic precipitate. Interestingly, DA autoxidation in aqueous buffer at pH 7.4, monitored through the characteristic DAC absorption at 475 nm, is partially quenched in SDS micelles (see Figure 11S). This is due to interaction of the protonated DA amino group with the negatively charged surface of the mimetic membrane,[25] which probably hinders intramolecular cyclization of DAQ to DAC.[24] The addition of catalytic amounts of Cu^{II} (25 μM) to a solution of DA (3 mM) in 50 mM Hepes buffer at pH 7.4 containing SDS (20 mM), increases its oxidation rate, and this slow catalytic effect is not affected by the addition of an excess Ac-αS_{1-15} (Figure 5A). Though, it is interesting that when the same experiment is carried out with αS_{1-15}, the non-acetylated peptide progressively quenches the reaction (Figure 5B).

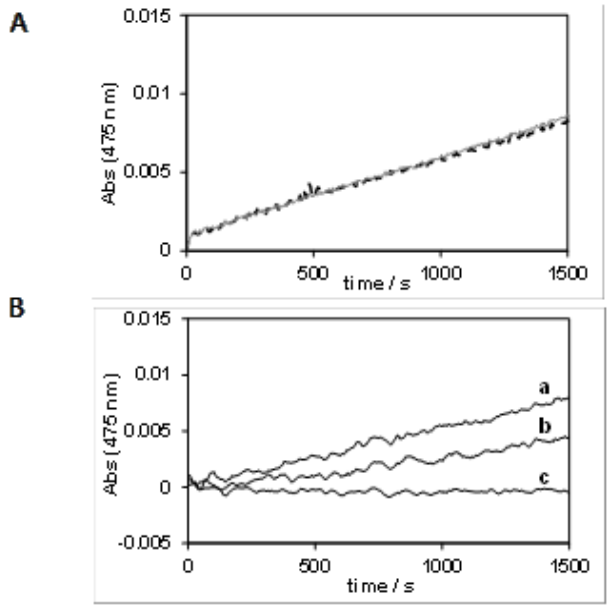

Figure 5. Kinetic profiles of DA oxidation with time, in 50 mM Hepes buffer solution at pH 7.4 and 25 °C with SDS (20 mM): (A) DA (3 mM) in the presence of Cu^{II} (25 μM) (gray line) and with addition of 2.5 equiv. of Ac-αS_{1-15} (black dotted line); (B) (a) DA (3 mM) in the presence of Cu^{II} (25 μM); (b) and (c): same as before but with addition of 1 and 2 equiv. of αS_{1-15}, respectively. In both cases, the absorption profiles were corrected for DA autoxidation in the same conditions.

These experiments suggest that the weak binding of Cu^{II} to Ac-αS_{1-15} is unable to keep the ion in the membrane (it is probably entirely bound to excess DA in the buffer solution). Upon reduction, Cu^{I} is not immediately trapped by Ac-αS_{1-15} in the membrane, because its reaction with O_2 is faster and catalytic turnover can proceed, as represented by the following simplified reaction scheme:

$$Cu^{II} + DA \rightarrow Cu^{I} + DA^{\cdot}$$

$$Cu^{I} + O_2 \rightleftarrows Cu/O_2$$

$$Cu/O_2 + DA \rightarrow\rightarrow Cu^{II} + DA^{\cdot}$$

$$2\,DA^{\cdot} \rightarrow DA + DAQ$$

On the contrary, αS_{1-15} binds strongly both Cu^{II} and Cu^{I} in the membrane, preventing the reaction of the latter with dioxygen. As a matter of fact, if Cu^{II} is reduced prior to the addition of DA and dioxygen, the resulting Cu^{I} ion is efficiently trapped by Ac-αS_{1-15} in nonreactive form in the membrane, so that DA oxidation is completely quenched (Figure 6).

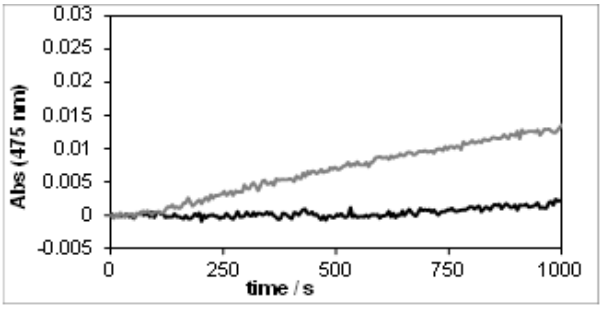

Figure 6. Kinetic profiles of DA oxidation with time, in 50 mM Hepes buffer solution at pH 7.4 and 25 °C with SDS (20 mM): DA (3 mM) in the presence of Cu^{II} (25 μM) and 2 equiv. of ascorbate (gray line), and with prior addition of 2.5 equiv. of Ac-αS_{1-15} (black line). The solutions containing SDS, ascorbate, Cu^{II} and peptide were prepared in an inert atmosphere and then an air-saturated solution of DA was added. Time zero corresponds to consumption of ascorbate.

Given the difficulties to carefully analyze DA oxidation products, we considered the oxidation of 4-methylcatechol (MC), which lacks functional groups in the side chain. As previously reported,[26] the oxidation of MC (3 mM) promoted by Cu^{II} (25 μM) at pH 7.4 (50 mM Hepes buffer) proceeds with a biphasic behavior due to the initial development of an absorption band at 401 nm (ε = 1550 M^{-1} cm^{-1}), due to 4-methylquinone (MQ), that subsequently shifts to 480 nm upon formation of an addition product between excess MC and the quinone. This addition product has been isolated and characterized here (Figure 12S and Scheme 1S). Longer reaction times lead to further oligomeric products that were not taken into consideration. When MC oxidation is studied in buffer containing SDS, the addition of slightly more than 2 equiv. Ac-αS_{1-15} with respect to Cu^{I} (generated by reduction of Cu^{II} with ascorbate before addition of the substrate) completely quenches the reaction (Figure 7). Note that SDS alone has no effect on the reactivity of free Cu^{II}.

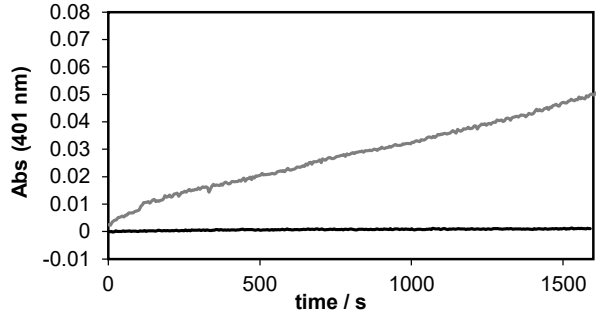

Figure 7. Kinetic profiles of MC oxidation with time, in 50 mM Hepes buffer solution at pH 7.4 and 25 °C with SDS (20 mM): MC (3 mM) in the presence of Cu^{II} (25 μM) and 2 equiv. of ascorbate (gray line), and with prior addition of 2.5 equiv. of Ac-$\alpha S_{1\text{-}15}$ (black line). The procedure is the same as that reported in the legend of Figure 4. The absorption profiles were corrected for MC autoxidation in the same conditions. Time zero corresponds to consumption of ascorbate.

On the other hand, the effect of $\alpha S_{1\text{-}15}$ on the copper mediated oxidation of MC is similar to that already observed for DA oxidation, i.e. the reaction is partially quenched by the high affinity of this peptide for Cu^{II} (Figure 8). More interestingly, if the medium also contains SDS the quenching is complete (Figure 8).

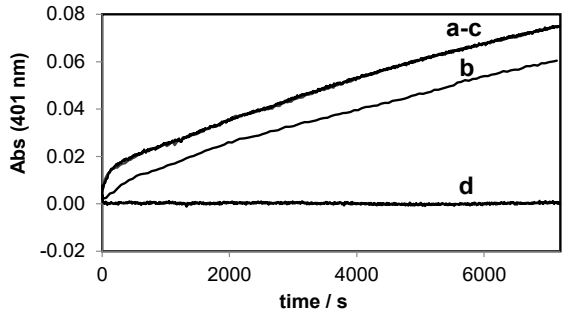

Figure 8. Kinetic profiles of MC oxidation (3 mM) in Hepes buffer (50 mM) at pH 7.4 and 25 °C in the presence of: (a) Cu^{II} (25 μM) alone, and with the addition of: (b) 2 equiv. of $\alpha S_{1\text{-}15}$; (c) SDS (20 mM); (d) 2 equiv. of $\alpha S_{1\text{-}15}$ and SDS (20 mM). All traces were corrected for MC autoxidation in the same conditions.

A more detailed study could be carried out using 3,5-di-*tert*-butylcatechol (DTBC), because it is electron-richer than DA and MC, and hence its oxidation is faster, and in addition it bears the advantage of forming a stable quinone (DTBQ). This allowed performing more detailed kinetic studies. The only drawback is that DTBC oxidation cannot be studied in pure aqueous buffer, due to its limited solubility.[27] The oxidation of this substrate (3 mM) in the presence of Cu^{II} (25 μM) was therefore studied in methanol/50 mM Hepes buffer at pH 7.4 (80:20 v/v), following the absorption band of DTBQ at 407 nm. As previously reported,[26] the addition of $\alpha S_{1\text{-}15}$ to the reaction solution leads to progressive reduction of the reaction rate, but the reaction is not completely quenched even at an $\alpha S_{1\text{-}15}$ to Cu^{II} ratio of 4:1 (Figure 9). However, when the experiment is carried out in the presence of SDS (20 mM), the quenching of the catalytic reaction becomes complete at ratio of $\alpha S_{1\text{-}15}$ to Cu^{II} ratio of 2:1 (Figure 9).

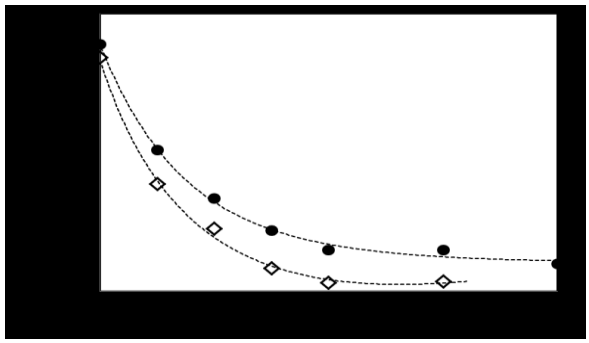

Figure 9. Dependence of the initial rate of DTBC oxidation on the molar ratio of $\alpha S_{1\text{-}15}/Cu^{II}$. The kinetics were studied in methanol/50 mM Hepes buffer at pH 7.4 (80:20 v/v) and 25 °C by reacting: (a) DTBC (3 mM), Cu^{II} (25 μM), and variable amounts of $\alpha S_{1\text{-}15}$, from 0 to 4 equiv. with respect to Cu^{II} (•), and (b) the reagents in the same conditions as above but with addition of SDS (20 mM) to the solution (◊).

The effect of Ac-$\alpha S_{1\text{-}15}$ in the catalytic DTBC oxidation in the presence of SDS depends on the initial copper oxidation state. When the experiment is performed starting with copper(II), the kinetic trace is not affected by the presence of Ac-$\alpha S_{1\text{-}15}$ (Figure 13S). This agrees with the low affinity of the acetylated peptide *vs.* copper(II). A different behavior is observed if the reaction is started from an anaerobic solution of copper(I). Upon exposure to air the DTBQ band progressively develops. But in the presence of Ac-$\alpha S_{1\text{-}15}$ the reactivity of copper is progressively reduced (Figure 10). This can be explained considering that Ac-$\alpha S_{1\text{-}15}$, maintains the copper(I) coordination set, therefore after binding the metal ion the resulting complex is transferred into the micelles. Most importantly, as in the case of DA oxidation, a complete quenching of the reaction is obtained with a Cu:Ac-$\alpha S_{1\text{-}15}$ = 1:2 molar ratio. The kinetic profiles of Figure 10 also show that upon copper redox cycling during turnover, the reactivity observed starting with copper(II) is restored. This does not happen when the copper:Ac-$\alpha S_{1\text{-}15}$ ratio is 1:2, suggesting that the $Cu^{I}(Ac\text{-}\alpha S_{1\text{-}15})_2$ species within the micelles is stable to dioxygen and unable to promote further oxidation.

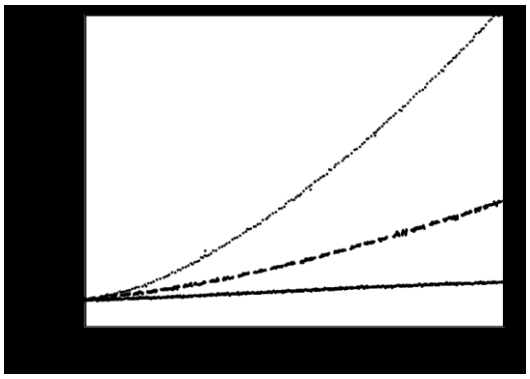

Figure 10 - Kinetic profiles at 407 nm for the oxidation of DTBC (3 mM) in methanol/50 mM Hepes buffer at pH 7.4 (80:20 v/v) and 25 °C in the presence of copper(I) (25 μM), stock solution in CH_3CN, and SDS (20 mM) (dotted line), and with the addition of: 1 equiv. of Ac-αSyn15 (dashed line); 2 equiv. of Ac-αS_{1-15} (black line). All traces were corrected for DTBC autoxidation in the same conditions.

CONCLUSIONS

The interaction of αS_{1-15} peptides, in both acetylated and non-acetylated forms, with membrane-like environment drastically changes their copper(I) binding ability, in terms of the donor atoms involved, binding stoichiometry, and affinity. The membrane-bound, α-helical αS peptides bind Cu^I in a 2:1 ratio yielding a tetrahedral CuS_4 site, through the side chains of the N-terminal methionines, and with higher affinity than the complex formed in aqueous solution.[19] αS_{1-15} peptides contain the copper binding sites of the full protein, suggesting that a similar behavior can be expected for full-length αS in the membrane, as previously demonstrated for unstructured αS. Therefore, it can be hypothesized that binding of the protein to the membrane not only represents a powerful trap for adventitious copper, which seems to be correlated with PD etiology,[28] but provides an excellent system for eliminating the potentially harmful redox reactivity of the metal ion.[18,29] In fact, unlike cytosolic Cu^I-αS, the membrane-bound complex may not promote oxidative reactions. This result can explain recent findings on cellular models, where it is shown that αS in physiological concentration and in its monomeric state does not generate ROS production and cell toxicity in the presence of copper or iron.[30] However, toxicity effects due to massive ROS production and oxidative stress arise when even small amounts of soluble αS oligomers are formed, at the early stages of the protein self-assembly process.

MATERIALS AND METHODS

1. Peptide synthesis. The N-terminal peptide fragment αS_{1-15} (^{1}MDVFMKGLSKAKEGV^{15}-NH_2) and its N-acetylated form Ac-αS_{1-15} (Ac-^{1}MDVFMKGLSKAKEGV^{15}-NH_2) were synthesized using the standard fluorenyl methoxycarbonyl (Fmoc) solid-phase synthesis in DMF. Rink-amide resin was used as solid support, which yielded the peptides amidated at the C-terminus. After deprotection of the resin with 20 mL of 20 % (v:v) piperidine in DMF, the first amino acid (3 mol equiv. *vs.* resin sites, estimated to be 0.64 mmol/g of resin), was added in the presence of 3 equiv. of *N*-hydroxybenzotriazole, 3 equiv. of benzotriazol-1-yl-oxytripyrrolidinophosphonium hexafluorophosphate and 6 equiv. of *N,N*-diisopropylethylamine. After 45 min, the same coupling procedure was repeated. After recoupling of each amino acid, a capping step was performed by using 20 mL of 4.7 % acetic anhydride and 4 % of pyridine in DMF. Deprotection of the Fmoc group was performed by treating twice the resin, for 3 min and 7 min, respectively, with 15 mL of 20 % piperidine in DMF. In order to obtain Ac-αS_{1-15} peptide the capping step procedure has been repeated also after the binding of the last residue, Met1.

At the end of the synthesis, the protection of the side chains of the amino acids were removed with a solution of 95 % trifluoroacetic acid (TFA, 25 ml for 1 g of resin), triisopropyl silane (2.5 %) and water (2.5 %), which serves also to release the peptide from the resin. After stirring for 3 h, the solution was concentrated under vacuum and cold diethyl ether was added to precipitate the peptide. The mixture was filtered and the precipitate washed with cold diethyl ether; then, it was dissolved in water and purified by HPLC, using a 0-100 % linear gradient of 0.1 % TFA in water to 0.1 % TFA in CH_3CN over 40 min (flow rate of 3 mL/min, loop 2 mL), as eluent. The product was then lyophilized, yielding a white solid, which was characterized by ESI-MS.

ESI-MS data (direct injection, MeOH, positive-ion mode, capillary temperature 200 °C): *m/z* 1640 ($\alpha S_{1-15}H^+$), 820 ($\alpha S_{1-15}H_2^{2+}$), 547 ($\alpha S_{1-15}H_3^{3+}$) a.m.u.; 1682 (Ac-$\alpha S_{1-15}H^+$), 841.5 (Ac-$\alpha S_{1-15}H_2^{2+}$), 561 (Ac-$\alpha S_{1-15}H_3^{3+}$) a.m.u.

2. CD spectroscopy. CD spectra were acquired on a Jasco J-815 spectropolarimeter at 288 K. A 0.1-cm cell path length was used for data between 180 and 260 nm, with a 1 nm sampling interval. Four scans were collected for every sample with scan speed of 100 nm min^{-1} and bandwidth of 1 nm. Baseline spectra were subtracted from each spectrum and data were smoothed with the Savitzky-Golay method.[31] Data were processed using Origin 5.0 spread sheet/graph package. The direct CD measurements (θ, in millidegrees) were converted to mean residue molar ellipticity, using the relationship: mean residue $\Delta\varepsilon = \theta/(33000 \times c \times l \times \text{number of residues})$, where c and l refer to molar concentration and cell path length, respectively. The CD spectra of αS_{1-15} in the presence of SDS is reported in Figure 1SA, whereas the CD titration of Ac-αS_{1-15} with Ag^I in the presence of SDS is reported in Figure 7S. The peptide concentration was 0.1 mM in 2.0 mM phosphate buffer at pH 7.4 and 25 °C. The desired concentrations of Ag^I ions and SDS were achieved by using stock solutions of $AgNO_3$ and SDS (Sigma Chemical Co.) in water.

3. NMR spectroscopy. NMR spectra were acquired at 298 K using Bruker Avance spectrometer operating at proton frequency of 600 MHz. NMR spectra were processed with XwinNMR 3.6 and TopSpin 3.0 software and

analyzed with the program Cara.[32] Suppression of residual water signal was achieved either by presaturation or by excitation sculpting,[33] using a selective 2 ms long square pulse on water. Proton resonance assignment of the peptides was obtained by 2D ^{1}H-^{1}H COSY, TOCSY and NOESY and ^{1}H-^{13}C HSQC experiments. The peptide was dissolved in 20 mM phosphate buffer at pH 7.4 with 10% of D_2O. The final peptide concentration was 0.4-0.5 mM. The desired concentrations of Ag^{I} ions and SDS were achieved by using stock solutions of $AgNO_3$ and SDS (Sigma Chemical Co.) in deuterated water. For Cu^{I} complexes, a 10 mM $[Cu(CH_3CN)_4]BF_4$ stock solution was prepared in 20 mM phosphate buffer in D_2O at pH 7.4 (containing 5% v/v CH_3CN). 1.5 mM ascorbic acid was added to the peptide just before use in order to avoid Cu^{I} oxidation to Cu^{II}. The relevant NMR data are reported in Figure 2S and 3S.

4. Structure Calculation. NOE cross peaks in 2D ^{1}H-^{1}H NOESY spectra acquired on apo peptides, Cu^{I}/Ag^{I} αS_{1-15} and Cu^{I}/Ag^{I} Ac-αS_{1-15} systems at 298 K were integrated with Cara program and were converted into internuclear distances list with the routine CALIBA of the program package DYANA.[34] To generate a NMR dimeric structure from a single distance restrains list, a double atom amino acid sequence of the same fragment was created in a single file, using the same distance restrains for both monomers. An ensemble of 30 structures were obtained by the standard protocol of simulated annealing in torsion angle space implemented in DYANA (using 10000 steps). To take into account the observed coordination behavior of the metal ion, distance constraints between metal and the two methionine sulfur donors of the two αS_{1-15} monomers were imposed (4 thioether groups coordinated), considering the 2:1 peptide metal ratio. No dihedral angle restraints and no hydrogen bond restraints were applied. The final structures were analyzed using the program MOLMOL.[35]

5. Kinetics of oxidation of catecholic substrates. The catalytic oxidation of catecholic substrates mediated by copper-Ac-αS_{1-15} or copper-αS_{1-15} complexes were studied in the presence of SDS and compared to that of free Cu^{2+}.

a) Dopamine oxidation

DA oxidation was monitored by UV-visible spectroscopy (with an Agilent 8453 spectrophotometer) through the absorption band of dopaminochrome at 475 nm.[36] DA (3 mM) autoxidation was studied in 50 mM 4-(2-hydroxyethyl)-1-piperazineethanesulfonic acid (Hepes) buffer at pH 7.4 at room temperature, in the absence and presence of SDS (20 mM) (Figure 11S).

The oxidation of DA in presence of αS_{1-15} (25-50 μM) or Ac-αS_{1-15} (62.5-100 μM) was studied using Cu^{II} (25 μM) in the presence of SDS (20 mM).

The copper(I) species was generated from copper(II) nitrate (25 μM), by reduction in an inert atmosphere with 2 equiv. of ascorbate. Thus, the solutions containing SDS, ascorbate, Cu^{II} and Ac-αS_{1-15} (62.5-100 μM) in Hepes buffer were prepared under an inert atmosphere in 2 mL volume and then the reaction was started by adding an air saturated solution of DA to obtain a final volume of 2.5 mL.

b) 4-Methylcatechol oxidation

MC oxidation was monitored through the absorption band of 4-methylquinone at 401 nm (ε = 1550 M^{-1} cm^{-1}),[26] that subsequently undergoes a shift to 480 nm due to an addition reaction by excess MC. The addition product has been characterized by ESI-MS: *m/z* 247 (addition product-H^{+}) a.m.u (Figure 12S). In Scheme 1S, the two isomeric compounds formed by nucleophilic attack of the catechol with quinone are shown.

The MC (3 mM) autoxidation experiment was performed in 50 mM Hepes buffer at pH 7.4 at room temperature in the absence and presence of SDS (20 mM). The catalytic oxidation of MC by Cu^{II}-αS_{1-15} was studied using copper(II) nitrate (25 μM) and αS_{1-15} (25-50 μM) in the presence and absence of SDS (20 mM).

The same study was performed with Cu^{I}-Ac-αS_{1-15}, using copper(II) nitrate (25 μM), after reduction in an inert atmosphere with 2 equiv. of ascorbate, and Ac-αS_{1-15} peptide (62.5-100 μM) and SDS (20 mM).

c) Kinetics of 3,5-Di-*tert*-butylcatechol oxidation

The oxidation of DTBC was monitored through the absorption band of DTBQ at 407 nm (ε = 1500 M^{-1} cm^{-1}), in a mixed solvent of 80% methanol and 20% 50 mM aqueous Hepes buffer at pH 7.4 (v/v) at 25 °C. All measurements were performed in duplicate. The kinetic traces showed a biphasic behavior. The conversion from $\Delta A/s$ to s^{-1} units was made using the quinone extinction coefficient and copper concentration. Autoxidation of the substrate was negligible in these conditions. To assess the effect of αS_{1-15} in the reaction, the peptide was added in variable stoichiometry (from 0 to 4 equivalents with respect to Cu^{2+}) in the presence of saturating concentration of DTBC (3 mM), followed by copper(II) nitrate (25 μM) as the last reagent. The same experiment was repeated in the presence of SDS (20 mM).

Similar studies were performed with the copper complex with Ac-αS_{1-15}. This peptide was added in variable stoichiometry (from 0 to 3 equivalents with respect to Cu) to a solution of 80% methanol and 20% 50 mM aqueous Hepes buffer at pH 7.4 (v/v) containing DTBC (3 mM), followed by tetrakis(acetonitrile)copper(I) hexafluorophosphate (25 μM, from a stock solution in MeCN) as the last reagent. The same experiment was repeated in the presence of SDS (20 mM).

ASSOCIATED CONTENT

Supporting Information. CD spectra and additional NMR spectra; binding plots; kinetic profiles of dopamine oxidation and 3,5-di-*tert*-butylcatechol; CPK graphical representation of the proposed Cu^{I} binding site; mass spectral characterization of oxidation product of 4-methyl catechol. This material is available free of charge via the Internet at http://pubs.acs.org.

AUTHOR INFORMATION

Corresponding Author

* luigi.casella@unipv.it

* daniela.valensin@unisi.it

ACKNOWLEDGMENT

This work was supported by the Italian MIUR, through the PRIN (Programmi di Ricerca di Rilevante Interesse Nazionale) project 2010M2JARJ_004. The COST CM1003 Action, CIRCMSB, and CIRMMP are also gratefully acknowledged.

REFERENCES

(1) Goedert, M. *Nat. Rev. Neurosci.* **2001**, *2*, 492-501.

(2) Spillantini, M. G.; Schmidt, M. L.; Lee, V. M.; Trojanowski, J. Q.; Jakes, R.; Goedert, M. *Nature* **1997**, *388*, 839-840.

(3) (a) Dawson, T. M.; Ko, H. S.; Dawson, V. L. *Neuron* **2010**, *66*, 646-661. (b) Devine, M. J.; Gwinn, K.; Singleton, A.; Hardy, J. *Movement Disorders* **2011**, *26*,2160-2168. (c) Lashuel, H. A.; Overk, C. R.; Oueslati, A.; Masliah, E. *Nat. Rev. Neurosci.* **2014**, *14*, 38-48.

(4) Hashimoto, M.; Takenouci, T.; Mallory, M.; Masliah, E.; Takeda, A. *Am. J. Pathol.* **2000**, *156*, 734-736.

(5) Iwai, A.; Masliah, E.; Yoshimoto, M.; Ge, N.; Flanagan, L.; de Silva, H. A.; Kittel, A.; Saitoh, T. *Neuron* **1995**, *14*, 467-475.

(6) Zhang, L.; Zhang, C.; Zhu, Y.; Cai, Q.; Chan, P.; Ueda, K.; Yu, S.; Yang, H. *Brain Res.* **2008**, *1244*, 40-52.

(7) Burre, J.; Sharma, M.; Tsetsenis, T.; Buchman, V.; Etherton, M.; Sudhof, T. C. *Science* **2010**, *329*, 1663-1667.

(8) (a) Binolfi, A.; Quintanar, L.; Bertoncini, C. W.; Griesinger C.; Fernández, C. O. *Coord. Chem. Rev.* **2012**, *256*, 2188-2201. (b) Carboni, E.; Lingor, P. *Metallomics* **2015**, *7*, 395-404.

(9) Anderson, J. P.; Walker, D. E.; Goldstein, J. M.; de Laat, R.; Banducci, K.; Caccavello, R. J.; Barbour, R.; Huang, J.; Kling, K.; Lee, M.; Diep, I.; Keim, P. S.; Shen, X.; Chataway, T.; Schlossmacher, M. G.; Seubert, P.; Schenk, D.; Sinha, S.; Gal, W. P.; Chilcote, T. J. *J. Biol. Chem.* **2006**, *281*, 29739-29752.

(10) (a) Castellani, R. J.; Siedlak, S. I.; Perry, G.; Smith, M. A. *Acta Neuropathol.* **2000**, *100*, 111-114. (b) Gaeta, A.; Hider, R. C. *Br. J. Pharmacol.* **2005**, *146*, 1041-1059.

(11) Pall, H. S.; Blake, D.R.; Gutteridge, J. M.; Williams, A. C.; Lumec, J.; Hall, M.; Taylor, A. *Lancet* **1987**, *2*, 238-241.

(12) (a) Hong, L.; Simon, J. D. *J. Phys. Chem. B* **2009**, *113*, 9551-9561. (b) Dudzik, C. G.; Walter, E. D.; Milhauser, G. L. *Biochemistry* **2011**, *50*, 1771-1777.

(13) Moriarty, G. M.; Minetti, C. A.; Remeta, D. P.; Baum, J. *Biochemistry* **2014**, *53*, 2815-2817.

(14) Miotto, M.; Valiente-Gabioud, A. A.; Rossetti, G.; Zweckstetter, M.; Carloni, P.; Selenko, P.; Griesinger, C.; Binolfi, A.; Fernandez, C. O. *J. Am. Chem. Soc.* **2015**, *137*, 6444-6447.

(15) (a) Ulmer, T. S.; Bax, A.; Cole, N. B.; Nussbaum, R. L. *J. Biol. Chem.* **2005**, *280*, 9595-9603. (b) Ulmer, T. S.; Bax, A. *J. Biol. Chem.* **2005**, *280*, 43179-43187. (c) Jao, C.; Hegde, B. G.; Chen, J.; Haworth, I. S.; Langen, R. *Proc. Natl. Acad. Sci. U. S. A.* **2008**, *105*, 19666-19671. (d) Bisaglia, M.; Mammi, S.; Bubacco, L. *FASEB J.* **2009**, *23*, 329-340.

(16) (a) Maltsev, A. S.; Ying, J.; Bax, A. *Biochemistry* **2012**, *51*, 5004-5013. (b) Dikiy, I.; Eliezer, D. *J. Biol. Chem.* **2014**, *289*, 3652-3665. (c) Bartels, T.; Kim, N. C.; Luth, E. S.; Selkoe, D. J. *PLOS One* **2014**, *9*, e103727.

(17) Dudzik, C. G.; Walter, E. D.; Abrams, B. S.; Jurica, M. S.; Milhauser, G. L. *Biochemistry* **2013**, *52*, 53-60.

(18) Zhou, B.; Hao, Y.; Wang, C.; Li, D.; Liu, Y.-N.; Zhou, F. *J. Inorg. Biochem.* **2013**, *118*, 68-73.

(19) (a) Camponeschi, F.; Valensin, D.; Tessari, I.; Bubacco, L.; Dell'Acqua, S.; Casella, L.; Monzani, E.; Gaggelli, E.; Valensin, G. *Inorg. Chem.* **2013**, *52*, 1358-1367. (b) Miotto, M.; Rodriguez, E. E.; Valiente-Gabioud, A. A.; Torres-Monserrat, V.; Binolfi, A.; Quintanar, L.; Zweckstetter, M.; Griesinger, C.; Fernandez, C. O.; *Inorg. Chem.* **2014**, *53*, 4350-4358. (c) De Ricco, R.; Valensin, D.; Dell'Acqua, S.; Casella, L.; Hureau, C.; Faller, P. *ChemBioChem*, **2015**, *16*, 2319-2328.

(20) (a) De Ricco, R.; Potocki, S.; Kozlowski, H.; Valensin, D. *Coord. Chem. Rev.* **2014**, *269*, 1-12. (b) De Ricco, R.; Valensin, D.; Dell'Acqua, S.; Casella, L.; Gaggelli, E.; Valensin, G.; Bubacco, L.; Mangani, S. *Inorg. Chem*., **2015**, *54*, 265-272.

(21) (a) Davies, P.; Wang, X.; Sarell, C. J.; Drewett, A.; Marken, F.; Viles, J. H.; Brown, D. R. *Biochemistry* **2011**, *50*, 37-47. (b) Chavarria, C.; Souza, J. M. *Arch. Biochem. Biophys.* **2013**, *533*, 25-32. (c) Wright, J. A.; Wang, X.; Brown, D. R. *FASEB J.* **2009**, *23*, 2384-2393. (d) Schildknecht, S.; Gerding, H. R.; Karreman, C.; Drescher, M.; Lashuel, H. A.; Outeiro, T. F.; Di Monte, D. A.; Leist, M. *J. Neurochem.* **2013**, *125*, 491-511.

(22) (a) Conway, K. A.; Lee, S. J.; Rochet, J. C.; Ding, T. T.; Williamson, R. E.; Lansbury Jr., P. T. *Science* **2001**, *294*, 1346-1349. (b) Rochet, J. C.; Outeiro, T. F.; Conway, K. A.; Ding, T. T.; Volles, M. J.; Lashuel, H. A.; Bieganski, R. M.; Lindquist, S. L.; Lansbury Jr., P. T. *J. Mol. Neurosci.* **2004**, *23*, 23-33. (c) Cappai, R.; Leck, S. L.; Tew, D. J. *FASEB J.* **2005**, *19*, 1377-1379. (d) Bisaglia, M.; Tosatto, L.; Munari, F.; Tessari, I.; de Laureto, P. P.; Mammi, S.; Bubacco, L. *Biochem. Biophys. Res. Commun.* **2010**, *394*, 424-428.

(23) Pham, A. N.; Waite, T. D. *J. Inorg. Biochem.* **2014**, *137*, 74-84.

(24) (a) Herlinger, E.; Jameson, R. F.; Linert, W.; *J. Chem. Soc. Perkin Trans. 2*, **1995**, 259-263. (b) Napolitano, A.; Manini, P.; d'Ischia, M. *Curr. Med. Chem.* **2011**, *18*, 1832-1845.

(25) Jodko-Piorecka, K.; Litwinienko, G. *ACS Chem. Neurosci.* **2013**, *4*, 1114-1122.

(26) Dell'Acqua, S.; Pirota, V.; Anzani, C.; Rocco, M. M.; Nicolis, S.; Valensin, D.; Monzani, E.; Casella, L. *Metallomics* **2015**, 7, 1091-1102.

(27) A. Granata, E. Monzani, L. Casella, *J. Biol. Inorg. Chem.* **2004**, *9*, 903-913

(28) Fukushima, T.; Tan, X.; Luo, Y.; Kanda, H. *Neuroepidemiology* **2011**, 36, 240-244.

(29) Wang, C.; Liu, L.; Zhang, L.; Peng, Y.; Zhou, F. *Biochemistry* **2010**, *49*, 8134-8142.

(30) Deas, E.; Cremades, N.; Angelova, P. R.; Ludtmann, M. H. R.; Yao, Z.; Chen, S.; Horrocks, M. H.; Banushi, B.; Little, D.; Devine, M. J.; Gissen, P.; Klenerman, D.; Dobson, C. M.; Wood, N. W.; Gandhi, S.; Abramov, A. Y. *Antiox. Redox Signal.* **2016**, *24*, 376-391.

(31) Savitzky, A.; Golay, M. J. E. *Anal. Chem.* **1964**, *36*, 1627-1639.

(32) Keller, R. W. K. http://www.nmr.ch.

(33) Hwang, T. L.; Shaka, A. J. *J. Magn. Res.* (San Diego, Calif.: 1997) **1998**, *135*, 280-287.

(34) Guntert, P.; Mumenthaler, C.; Wuthrich, K. *J. Mol. Biol.* **1997**, *273*, 283-298.

(35) Koradi, R.; Billeter, M.; Wuthrich, K. *J. Mol. Graphics* **1996**, *14*, 51-55.

(36) Herlinger, E.; Jameson, R. F.; Linert, W. *J. Chem. Soc. Perkin Trans.* **1995**, *2*, 259-263.

SYNOPSIS TOC

In a membrane environment, copper(I) binds to the truncated α-synuclein (αS) peptide 1-15, both in N-acetylated and free amine forms, with a 1:2 Cu^{I}-αS stoichiometry, where Cu^{I} is bound to Met1 and Met5 residues of two helical peptide chains. The resulting tetrahedral Cu^{I} center is redox stable, does not form reactive oxygen species, and is unreactive against dopamine in the presence of O_2.

Insert Table of Contents artwork here